frontiers in Materials

ORIGINAL RESEARCH
published: 24 September 2020
doi: 10.3389/fmats.2020.00262

Hypothetical $P6_3/mmc$-Type $CsCrCl_3$ Ferromagnet: Half-Metallic Property and Nodal Surface State

Yang Li[1,2]*

[1] Faculty of Mechanical and Electrical Engineering, Kunming University of Science and Technology, Kunming, China,
[2] Department of Physics, Chongqing University of Arts and Sciences, Chongqing, China

This work focuses on the electronic, magnetic, and half-metallic behaviors and interesting surface state of a hypothetical $CsCrCl_3$ ferromagnet with a $P6_3/mmc$ space group, investigated using the spin-polarized generalized gradient approach (GGA) and spin-polarized GGA plus Hubbard U correction within the framework of density functional theory. The calculated total magnetic moment of $P6_3/mmc$ $CsCrCl_3$ is ∼7.397 μ_B, and the main contribution to the total magnetism is from the Cr atoms. Based on the obtained spin-polarized band structures, we confirm that this hypothetical $CsCrCl_3$ ferromagnet is a half-metal with 100% spin-polarization. Without spin-orbit coupling, i.e., when the spin and orbit degrees of freedom are dependent, we found an interesting nodal surface state at the $k_z = \pi$ plane due to the $P6_3/mmc$ type lattice structure having a twofold screw axis S_{2z}. Our study provides strong evidence that a protected nodal surface state can be achieved in magnetic materials.

Keywords: DFT, half-metallic materials, band gap, nodal surface properties, electronic structure

OPEN ACCESS

Edited by:
Zhenxiang Cheng,
University of Wollongong, Australia

Reviewed by:
Biao Wang,
Southwest University, China
Guangqian Ding,
Chongqing University of Posts and Telecommunications, China
Xiaoming Zhang,
Hebei University of Technology, China

***Correspondence:**
Yang Li
liyang@cqwu.edu.cn;
liyang_physics@126.com

Specialty section:
This article was submitted to Computational Materials Science, a section of the journal Frontiers in Materials

Received: *06 June 2020*
Accepted: *17 July 2020*
Published: *24 September 2020*

Citation:
Li Y (2020) Hypothetical $P6_3/mmc$-Type $CsCrCl_3$ Ferromagnet: Half-Metallic Property and Nodal Surface State. Front. Mater. 7:262. doi: 10.3389/fmats.2020.00262

INTRODUCTION

The search for half-metallic materials (De Groot et al., 1983; Pickett and Moodera, 2001; Elfimov et al., 2002; Kusakabe et al., 2004; Zhang et al., 2018) with 100% spin-polarization (P) (Žutic et al., 2004) is a hot research topic in next-generation spintronics (Li and Yang, 2016). Half-metallic materials (Ding and Wang, 2016; Hu et al., 2017; Wang et al., 2017; Wu et al., 2017; Bhattacharyya et al., 2018; Du et al., 2019; Huang et al., 2019; Wang et al., 2019; Zhang et al., 2019) are so called owing to their unique electronic band structures in both spin channels: the bands in one spin channel exhibit a metallic property, whereas those in the other spin channel have semiconducting or insulating behaviors. Therefore, based on the formula: $P = \frac{n\uparrow(E_F)-n\downarrow(E_F)}{n\uparrow(E_F)+n\downarrow(E_F)} \times 100\%$, where ($n \uparrow (E_F)$ and $n \downarrow (E_F)$ are the spin-up density of states (DOS) and the spin-down DOS at the Fermi level (E_F), respectively, the half-metallic materials should have 100% P in theory. Notably, half-metallic materials are good spin injectors into semiconductors, with maximum efficiency in spintronics devices. Various families of materials, including Heusler alloys (Kandpal et al., 2007; Wang et al., 2015; Cui et al., 2019; Han et al., 2019; Singh and Gupta, 2019), metallic oxides (Szotek et al., 2004), perovskite compounds (Li et al., 2015), wurtzite compounds (Wu et al., 2006), nanowires (Li et al., 2017), nanoribbons (Son et al., 2006), and some two-dimensional (2D) monolayers (Gao et al., 2016; Ashton et al., 2017; Feng et al., 2018; Liu et al., 2019), have been predicted to be half-metallic materials. Half-metals can be used for pure spin generation and injection. To develop practicable spintronic devices using half-metals, the spin-flip (half-metallic gap) should be wide enough to prevent thermally agitated spin-flip transition and preserve half-metallicity.

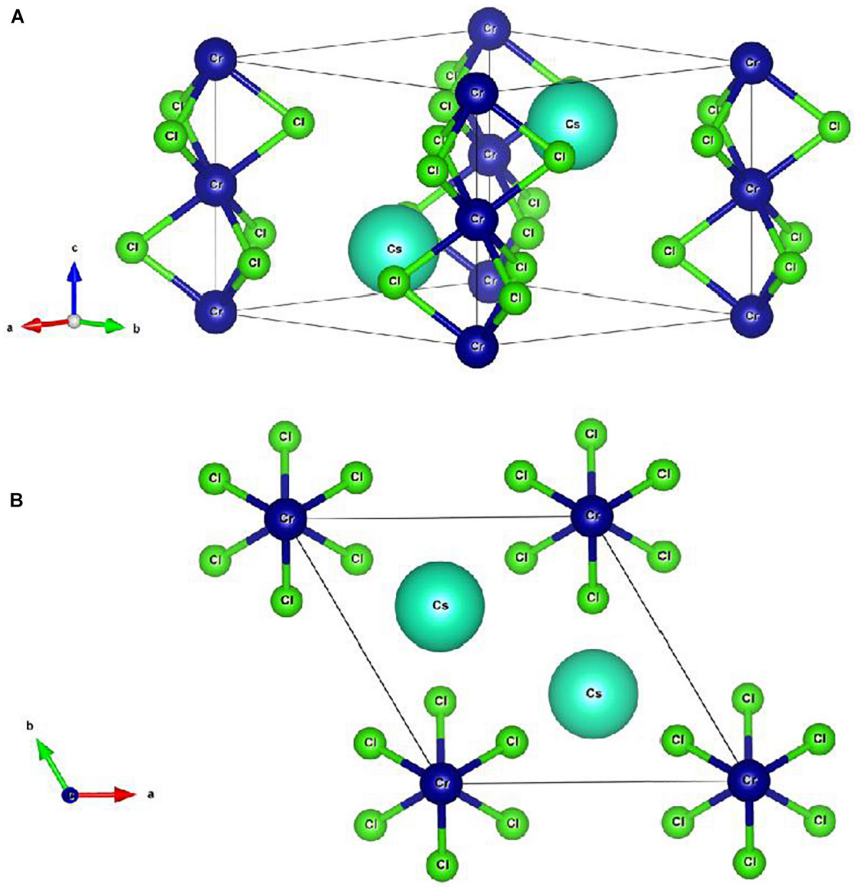

FIGURE 1 | Crystal model of $CsCrCl_3$ from different perspectives **(A,B)**.

Wu et al. (2018) proposed a new class of topological bulk materials, 3D nodal surface semimetals. They are topological materials with 2D nodal surface states, which are different from topological semimetals with a 0D nodal point (Soluyanov et al., 2015; Young and Kane, 2015; Kumar et al., 2017; Jin K. et al., 2019) and 1D nodal line (Chen et al., 2018; Liu et al., 2018; Zhou et al., 2018; He et al., 2019; Jin L. et al., 2019; Pham et al., 2019; Yan et al., 2019; Yi et al., 2019; Zou et al., 2019; Zhao et al., 2020). To date, only a few nodal surface semimetals (Wu et al., 2018) have been the subject of theoretical investigations. Nodal surface semimetals have a 2D nodal surface state composed of numerous band-crossing points. That is, each point on the surface is an intersection point between the two bands, and its dispersion is linear along the surface normal direction. Coarse-grained quasiparticles excited from a nodal surface effectively behave as 1D massless Dirac fermions along the surface normal direction and may show novel physical behaviors.

In this work, we use density functional theory (DFT) calculations to systematically investigate the electronic, magnetic, and half-metallic properties of the hypothetical $CsCrCl_3$ ferromagnet, as well as a topological nodal surface signature, with respect to its potential applications in next-generation spintronics and electronics devices. We predict that the hypothetical $CsCrCl_3$ ferromagnet is a novel material co-featuring a half-metallic property and nodal surface state at the $k_z = \pi$ plane. The formation energy of the ferromagnetic type $CsCrCl_3$ with $P6_3/mmc$ space group and 194 space

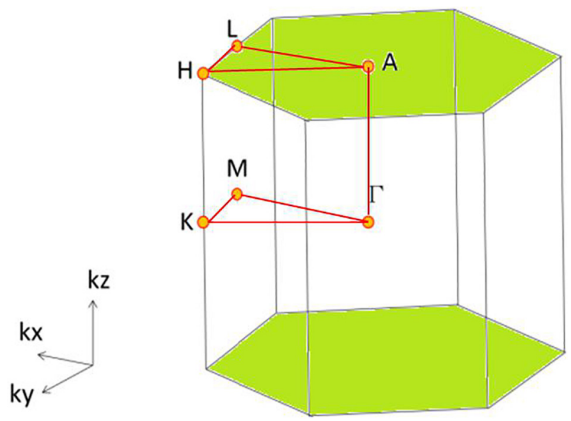

FIGURE 2 | Selected high-symmetry points in the first Brillouin zone. The $k_z = \pi$ plane is shown in green.

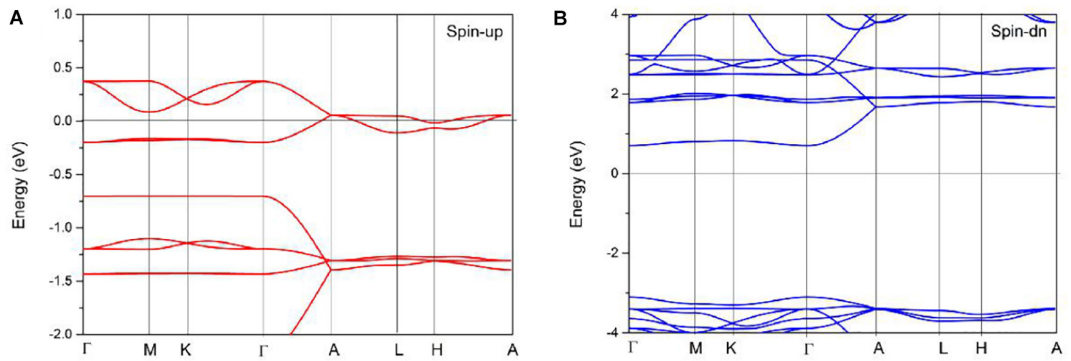

FIGURE 3 | Spin-polarized band structures of $CsCrCl_3$ system via GGA method. **(A)** for spin-up and **(B)** for spin-down.

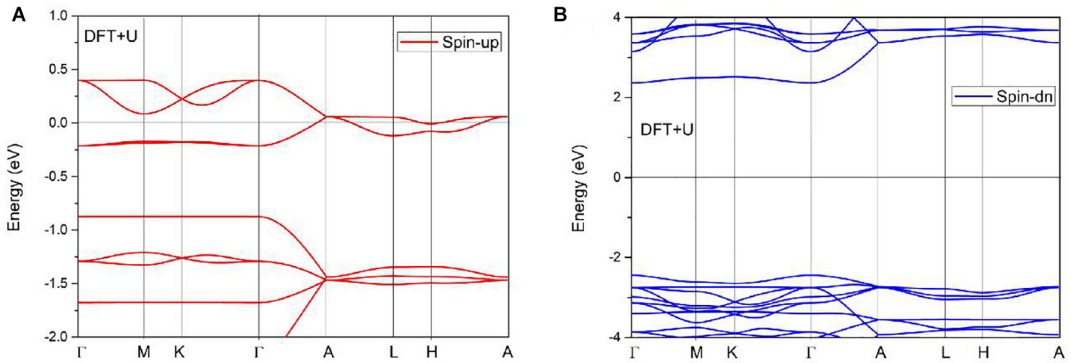

FIGURE 4 | Spin-polarized band structures of $CsCrCl_3$ system via DFT + *U* method. **(A)** for spin-up and **(B)** for spin-down.

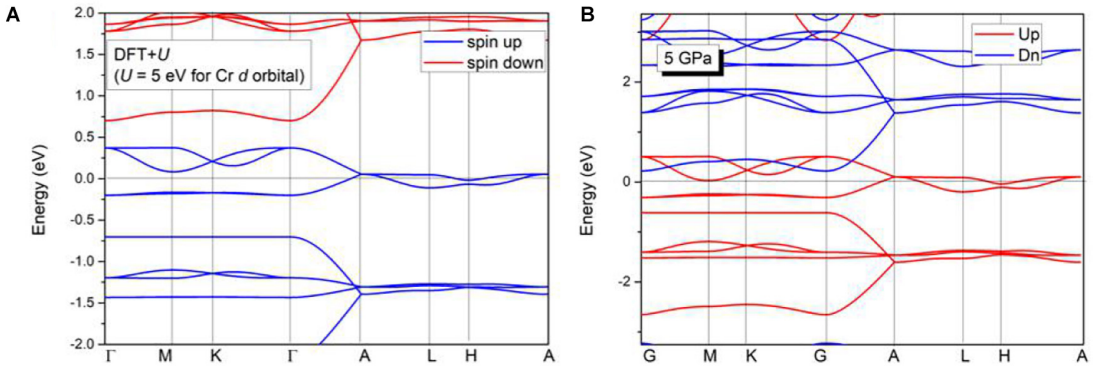

FIGURE 5 | Spin-polarized band structures of $CsCrCl_3$ system with DFT + *U* method **(A)** and with uniform strain **(B)**, respectively.

number was calculated to be -1.736 eV in https://www.materialsproject.org/materials/mp-570326/, indicating that this hexagonal ferromagnet is theoretically stable.

COMPUTATIONAL DETAILS

All atomic and electronic structure calculations were performed using the Vienna *ab initio* simulation package (Sun et al., 2003) with generalized gradient approximation (GGA) (Perdew et al., 1996) using the Perdew–Burke–Ernzerhof (Perdew et al., 1998) exchange-correlation functional. The projector augmented wave pseudo-potential was employed, with a cutoff energy of 600 eV for plane-wave expansions and a Monkhorst–Pack special $5 \times 5 \times 9$ k-point mesh. The convergence criteria for energy and force were set to 10^{-6} eV per atom and 0.0005 eV/Å, respectively. For the $CsCrCl_3$ material, we considered strong correlation effects in the transition-metal Cr atoms. The Hubbard

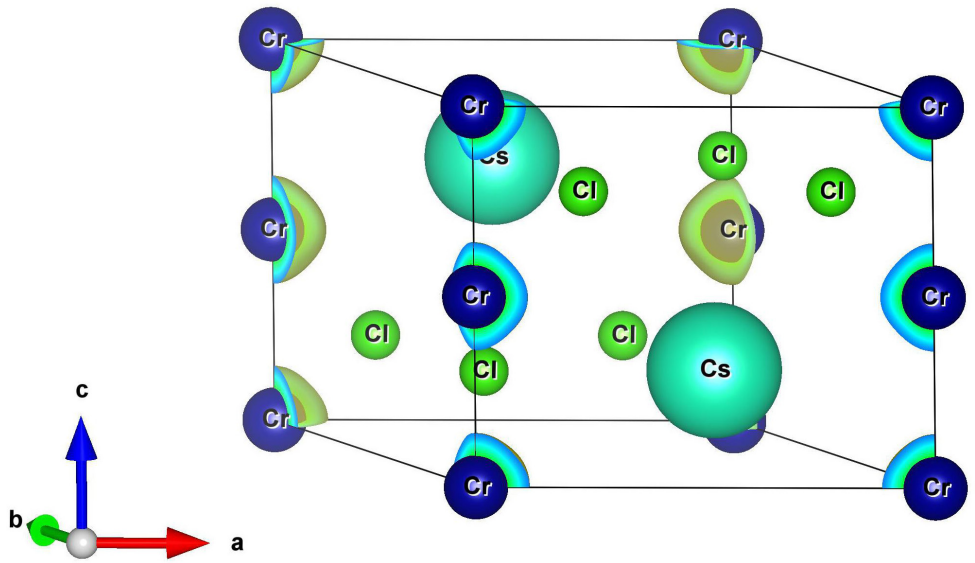

FIGURE 6 | Spin-density for the $CsCrCl_3$ ferromagnet.

U correction was also used in the rotationally invariant DFT + *U* approach to further confirm the band structure.

RESULTS AND DISCUSSION

The crystal structure of $CsCrCl_3$ from different perspectives is given in **Figures 1A,B**, respectively. $CsCrCl_3$ has a $BaVS_3$ type hexagonal structure, with a $P6_3/mmc$ space group and a space number of 194. As shown in **Figure 1**, the Cr atoms are surrounded by octahedrons of Cl atoms, which form 1D chains along the *z*-axis and share common faces. These chains are arranged in a trigonal lattice in the *x*-*y* plane, with Cs atoms inserted between the chains. We fully optimized the crystal model (**Figure 1**), and the obtained equilibrium lattice constants for the $CsCrCl_3$ ferromagnet were a = b = 7.40130 Å and c = 6.1870 Å. Our calculated results were in good agreement with those in the materials project database[1] (a = b = 7.395 Å, c = 6.173 Å) and topological materials database[2] (a = b = 7.249 Å, c = 6.228 Å).

Based on the obtained equilibrium lattice constants, we studied the electronic band structures of the $CsCrCl_3$ ferromagnet. The Γ-M-K-Γ-A-L-H-A high-symmetry points (**Figure 2**) in the first Brillouin zone were selected to describe the spin-polarized band structures of the $CsCrCl_3$ ferromagnet. The spin-up and spin-down band structures were calculated using the GGA method and the results are shown in **Figures 3A,B**, respectively. One can see that the spin-up electronic bands and the E_F overlapped with each other, reflecting the metallic property. For the spin-down channel, a clear band gap appeared, indicating the semiconducting behavior. Moreover, the values of the band gap and half-metallic gap (Guo et al., 2016; Wang et al., 2016) were calculated to be 3.78 and 0.7 eV, respectively, indicating that the half-metallic state of the $CsCrCl_3$ system is very robust. To properly account for the strong correlation effects in the transition-metal Cr atoms, a Hubbard *U* correction was adopted in the rotationally invariant DFT + *U* approach. In **Figure 4**, the spin-polarized band structures obtained via the DFT + *U* method (*U* = 3 eV for Cr-*d* orbitals) are shown. One can see that the half-metallic state for this $CsCrCl_3$ system was retained. That is, the metallic state and semiconducting state, in the spin-up and spin-down directions, respectively, could still be observed. However, the band gap and the half-metallic band gap in the spin-down channel increased to values of 4.496 and 2.375 eV, respectively.

Furthermore, we would like to point out that the half-metallic states of the $CsCrCl_3$ ferromagnet are very robust to the Hubbard *U* correction and the uniform strain. In **Figure 5**, the band structures of the $CsCrCl_3$ ferromagnet with *U* = 5 eV for Cr-*d* orbitals and with 5 GPa uniform strain, respectively, are given. One can see that the $CsCrCl_3$ ferromagnet still hosts half-metallic properties under the above-mentioned situations.

The primitive cell of the $CsCrCl_3$ ferromagnet contained eight atoms, i.e., two Cr atoms, two Cs atoms, and six Cl atoms. The total magnetic moment for this system was 7.397 μ_B, and the atomic magnetic moments of Cr atoms (~3.693 μ_B) dominated the total magnetism. To further examine the magnetism of this system, the spin-density in both spin channels was determined (**Figure 6**). The spin-density was mainly located around the Cr atoms, indicating that they have large atomic magnetic moments.

[1]https://www.materialsproject.org/materials/mp-570326/

[2]https://www.topologicalquantumchemistry.org/#/detail/36132

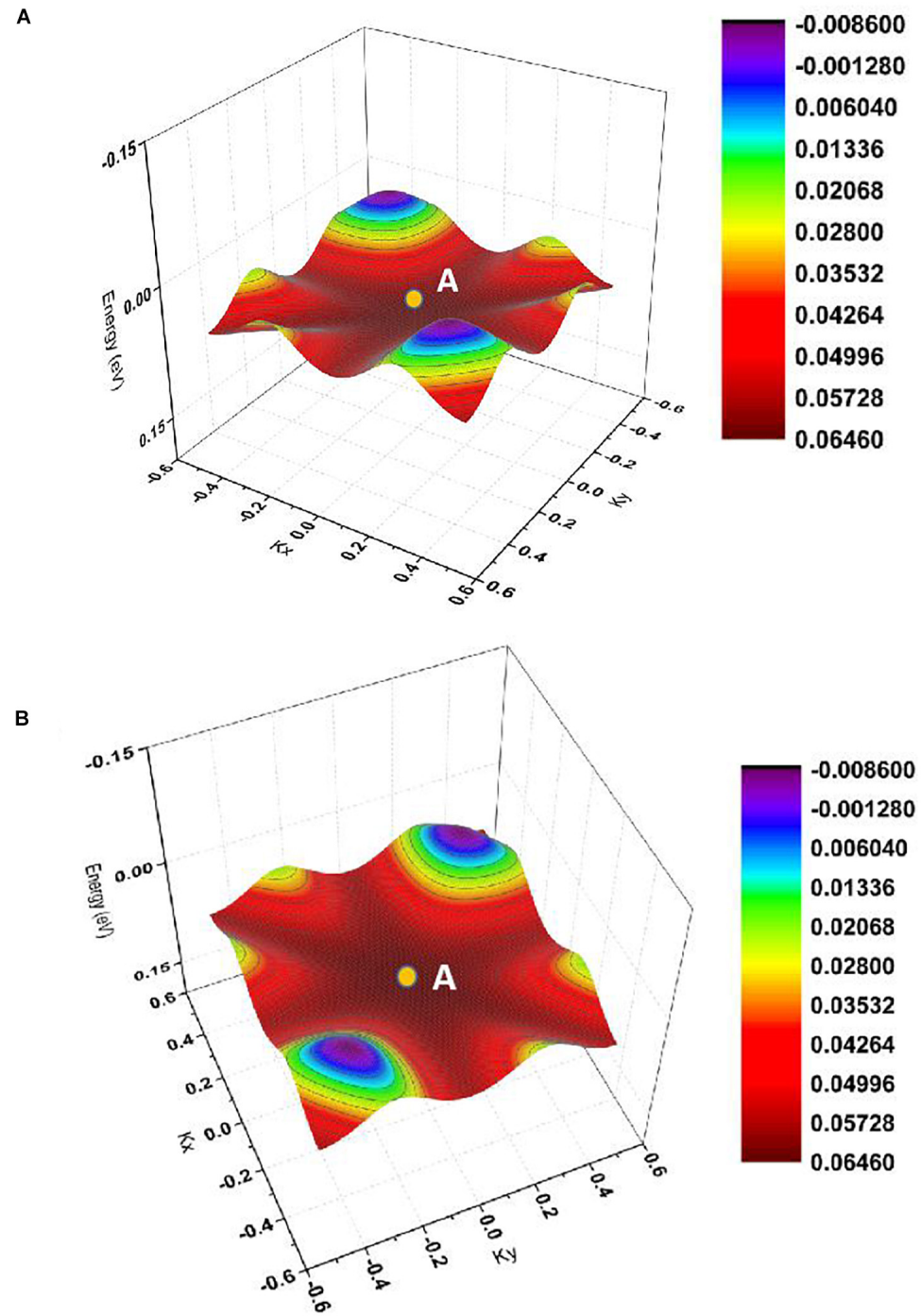

FIGURE 7 | A-point centered 3D band structures of $CsCrCl_3$ ferromagnet at $k_z = \pi$ plane in spin-up channel (without SOC effect). **(A,B)** are from different view sides.

The contributions of other atoms, including Cs and Cl atoms, to the total magnetism were almost negligible.

Note that the spin-orbit coupling (SOC) effect was not considered in this work. Without SOC, the spin and orbit degrees of freedom are independent; therefore, the spin degree and the orbit degree can be regarded as different subspaces (Wu et al., 2018). With a selected spin-polarization axis, the spin-up and spin-down directions are decoupled; therefore, the bands for each spin species can be effectively seen as for a spin-free system. Thus, the protected nodal surface state can be realized in one spin of a ferromagnet when the SOC effect is neglected. As shown in **Figure 3**, along the A-L-H-A direction, two bands (in the range

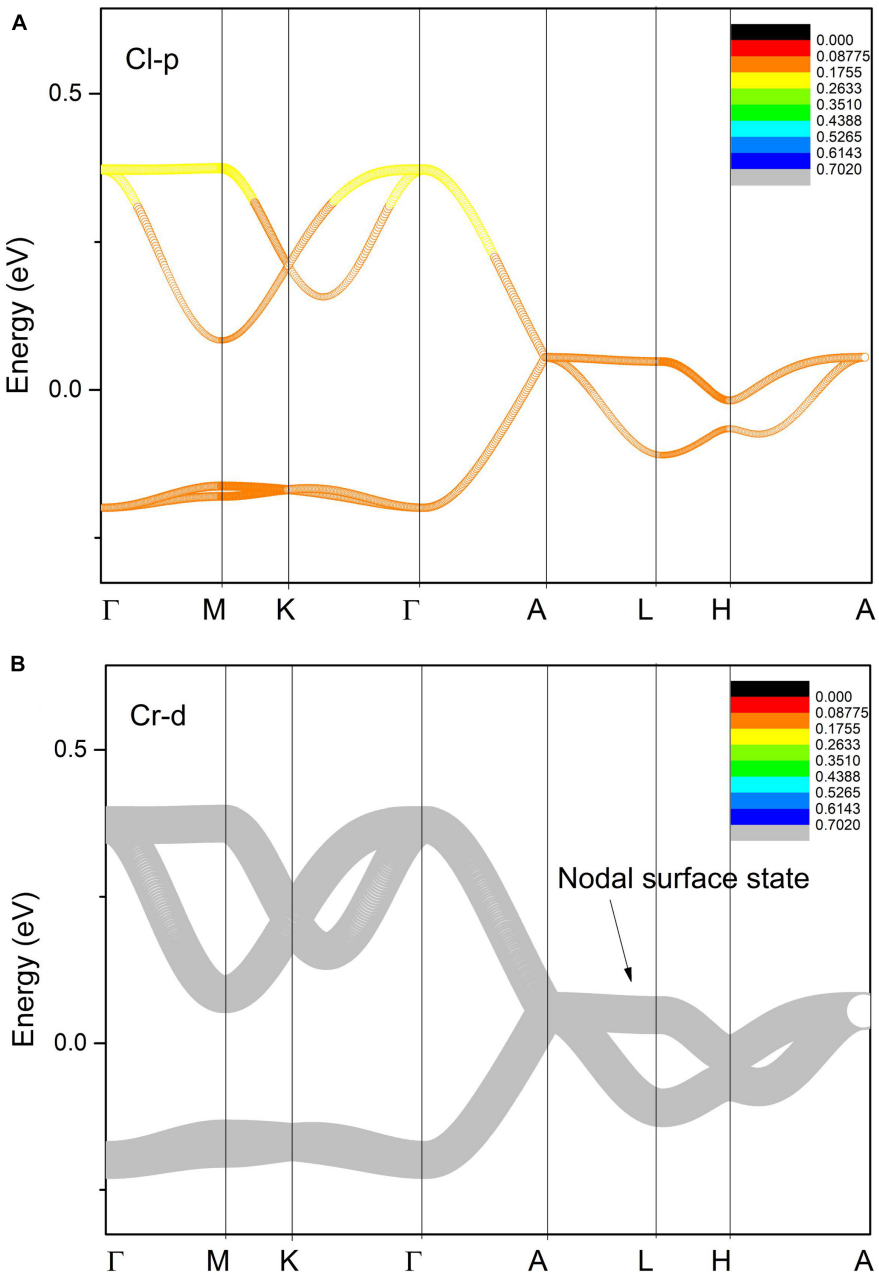

FIGURE 8 | Orbital-resolved band structures of Cl-*p* **(A)** and Cr-*d* **(B)** orbitals of $CsCrCl_3$ in the spin-up channel. The nodal surface state, formed by the crossing of two bands near the E_F, is highlighted by an arrow along the A-L-H-A direction.

of -0.1 to 0.1 eV) were totally degenerate with each other. The lattice structure of the $CsCrCl_3$ ferromagnetic system features a 2-fold screw axis S_{2z}. As discussed by Wu et al. (2018), a nodal surface state (at the $k_z = \pi$ plane) must occur in the ferromagnetic material if the crystal structure of the ferromagnetic material hosts a 2-fold screw axis S_{2z}. To further investigate whether there was a nodal surface state in this $CsCrCl_3$ system, the 3D band structure (A-point-centered) in the spin-up channel was examined from different perspectives. In **Figures 7A,B**, one can see that a nodal surface state existed in the $k_z = \pi$ plane near the E_F. Furthermore, one can see that the nodal surface state (at the $k_z = \pi$ plane and in the spin-up channel) was relatively flat in energy, that is, the energy variation was less than 0.2 eV. Finally, in **Figure 8**, the calculated orbital-resolved band structures of the Cl-*p* and Cr-*d* orbitals states are shown. The orbital-resolved band structure of the Cs-s orbitals is not shown, as it had little effect on the nodal surface state near the E_F in the spin-up channel. The main contribution to the nodal surface state was from the Cr-*d* orbits; however, the contribution of the Cl-*p* orbitals was not negligible.

CONCLUSION

In conclusion, in this study, a hypothetical $CsCrCl_3$ ferromagnetic system with a $P6_3/mmc$ space group and a space number of 197 was investigated in detail with respect to its electronic structures, magnetism, half-metallic behavior, and topological signature via DFT and DFT + U. We predict that the $CsCrCl_3$ ferromagnet is an excellent half-metal with a large band gap and a half-metallic gap. Moreover, this $CsCrCl_3$ ferromagnet has a nodal surface state (at the $k_z = \pi$ plane) in the spin-up channel when the SOC effect is not taken into consideration. The nodal surface state in the spin-up channel is due to the $P6_3/mmc$ lattice structure, which features a twofold screw axis S_{2z}. Based on the spin-density and the orbital-resolved band structure, we confirmed that the main contribution to the total magnetism and the surface state near the E_F was from the Cr-d orbitals. It is hoped that our theoretical work will inspire further research to explore the half-metallic behaviors and the nodal surface states of many other materials in the future.

DATA AVAILABILITY STATEMENT

All datasets presented in this study are included in the article/supplementary material.

AUTHOR CONTRIBUTIONS

The author confirms being the sole contributor of this work and has approved it for publication.

FUNDING

This work was supported by the first batch of post-doctoral research fund research projects in Yunnan Province (Serial No. 9), the Science and Technology Research Program of Chongqing Municipal Education Commission (Grant No. KJQN201801346), and the Chongqing University of Arts and Sciences Foundation (Grant No. Z2011Rcyj05).

REFERENCES

Ashton, M., Gluhovic, D., Sinnott, S. B., Guo, J., Stewart, D., and Hennig, R. G. (2017). Two-dimensional intrinsic half-metals with large spin gaps. *Nano Lett.* 17, 5251–5257. doi: 10.1021/acs.nanolett.7b01367

Bhattacharyya, G., Choudhuri, I., and Pathak, B. (2018). High Curie temperature and half-metallicity in an atomically thin main group-based boron phosphide system: long range ferromagnetism. *Phys. Chem. Chem. Phys.* 20, 22877–22889. doi: 10.1039/c8cp03440k

Chen, H., Zhang, S., Jiang, W., Zhang, C., Guo, H., Liu, Z., et al. (2018). Prediction of two-dimensional nodal-line semimetals in a carbon nitride covalent network. *J. Mater. Chem. A* 6, 11252–11259. doi: 10.1039/c8ta02555j

Cui, Z., Wu, B., Ruan, X., Zhou, Q., Liu, Z., Fu, X., et al. (2019). Enhancing the half-metallicity of equiatomic quaternary Heusler compound CoFeCrGe via atomic doping. *Results Phys.* 15:102533. doi: 10.1016/j.rinp.2019.102533

De Groot, R., Mueller, F. M., Van Engen, P. G., and Buschow, K. H. (1983). New class of materials: half-metallic ferromagnets. *Phys. Rev. Lett.* 50, 2024–2027. doi: 10.1103/physrevlett.50.2024

Ding, Y., and Wang, Y. (2016). Enhanced piezoelectricity and half-metallicity of fluorinated AlN nanosheets and nanoribbons: a first-principles study. *J. Mater. Chem. C* 4, 1517–1526. doi: 10.1039/c5tc03910j

Du, Y., Bu, H., Ji, C., Zhang, X., Li, C., and Fang, X. (2019). Tunable magnetic and half-metallic properties of the two-dimensional electron gas in LaAlO3/SrTiO3(111) heterostructures. *Phys. Chem. Chem. Phys.* 21, 18170–18178. doi: 10.1039/c9cp00746f

Elfimov, I. S., Yunoki, S., and Sawatzky, G. A. (2002). Possible path to a new class of ferromagnetic and half-metallic ferromagnetic materials. *Phys. Rev. Lett.* 89:216403.

Feng, Y., Wu, X., Han, J., and Gao, G. (2018). Robust half-metallicities and perfect spin transport properties in 2D transition metal dichlorides. *J. Mater. Chem. C* 6, 4087–4094. doi: 10.1039/c8tc00443a

Gao, G., Ding, G., Li, J., Yao, K., Wu, M., and Qian, M. (2016). Monolayer MXenes: promising half-metals and spin gapless semiconductors. *Nanoscale* 8, 8986–8994. doi: 10.1039/c6nr01333c

Guo, R., Liu, G., Wang, X., Rozale, H., Wang, L., Khenata, R., et al. (2016). First-principles study on quaternary Heusler compounds ZrFeVZ (Z = Al, Ga, In) with large spin-flip gap. *RSC Adv.* 6, 109394–109400. doi: 10.1039/c6ra18873g

Han, Y., Chen, Z., Kuang, M., Liu, Z., Wang, X., and Wang, X. (2019). 171 Scandium-based full Heusler compounds: a comprehensive study of competition between XA and L21 atomic ordering. *Results Phys.* 12, 435–446. doi: 10.1016/j.rinp.2018.11.079

He, T., Zhang, X., Meng, W., Jin, L., Dai, X., and Liu, G. (2019). Topological nodal lines and nodal points in the antiferromagnetic material β-Fe2PO5. *J. Mater. Chem. C* 7, 12657–12663. doi: 10.1039/c9tc04046c

Hu, R., Zhang, Z. H., and Fan, Z. Q. (2017). BN nanoflake quantum-dot arrays: structural stability, and electronic and half-metallic properties. *Phys. Chem. Chem. Phys.* 19, 20137–20146. doi: 10.1039/c7cp02391j

Huang, H. M., Cao, M., Jiang, Z., Xiong, Y., Zhang, X., Luo, S., et al. (2019). High spin polarization in formamidinium transition metal iodides: first principles prediction of novel half-metals and spin gapless semiconductors. *Phys. Chem. Chem. Phys.* 21, 16213–16222. doi: 10.1039/c9cp00958b

Jin, K., Huang, H., Wang, Z., and Liu, F. (2019). A 2D nonsymmorphic Dirac semimetal in a chemically modified group-VA monolayer with a black phosphorene structure. *Nanoscale* 11, 7256–7262. doi: 10.1039/c9nr00906j

Jin, L., Zhang, X., He, T., Meng, W., Dai, X., and Liu, G. (2019). Topological nodal line state in superconducting NaAlSi compound. *J. Mater. Chem. C* 7, 10694–10699. doi: 10.1039/c9tc03464a

Kandpal, H. C., Fecher, G. H., and Felser, C. (2007). Calculated electronic and magnetic properties of the half-metallic, transition metal based Heusler compounds. *J. Phys. D Appl. Phys.* 40, 1507–1523. doi: 10.1088/0022-3727/40/6/s01

Kumar, N., Sun, Y., Xu, N., Manna, K., Yao, M., Suss, V., et al. (2017). Extremely high magnetoresistance and conductivity in the type-II Weyl semimetals WP2 and MoP2. *Nat. Commun.* 8, 1–8.

Kusakabe, K., Geshi, M., Tsukamoto, H., and Suzuki, N. (2004). New half-metallic materials with an alkaline earth element. *J. Phys. Condens. Matter.* 16:S5639.

Li, M., Retuerto, M., Deng, Z., Stephens, P. W., Croft, M., Huang, Q., et al. (2015). Giant magnetoresistance in the half-metallic double-perovskite ferrimagnet Mn2FeReO6. *Angew. Chem.* 54, 12069–12073. doi: 10.1002/anie.201506456

Li, X., Lv, H., Dai, J., Ma, L., Zeng, X. C., Wu, X., et al. (2017). Half-metallicity in one-dimensional metal trihydride molecular nanowires. *J. Am. Chem. Soc.* 139, 6290–6293. doi: 10.1021/jacs.7b01369

Li, X., and Yang, J. (2016). First-principles design of spintronics materials. *Natl. Sci. Rev.* 3, 365–381. doi: 10.1093/nsr/nww026

Liu, J., Li, X., Wang, Q., Kawazoe, Y., and Jena, P. (2018). A new 3D Dirac nodal-line semi-metallic graphene monolith for lithium ion battery anode materials. *J. Mater. Chem.* 6, 13816–13824. doi: 10.1039/c8ta04428g

Liu, Y., Guo, S., Yu, J., and Zhong, H. (2019). Large magnetoresistance and perfect spin filter effect in Fe doped SnS2 half-metallic monolayers: a first principles study. *Phys. Lett. A* 383, 674–679. doi: 10.1016/j.physleta.2019.01.008

Perdew, J. P., Burke, K., and Ernzerhof, M. (1996). Generalized gradient approximation made simple. *Phys. Rev. Lett.* 77:3865. doi: 10.1103/physrevlett.77.3865

Perdew, J. P., Burke, K., and Ernzerhof, M. (1998). Perdew, burke, and ernzerhof reply. *Phys. Rev. Lett.* 80:891. doi: 10.1103/physrevlett.80.891

Pham, A., Klose, F., and Li, S. (2019). Robust topological nodal lines in halide carbides. *Phys. Chem. Chem. Phys.* 21, 20262–20268. doi: 10.1039/c9cp04330f

Pickett, W. E., and Moodera, J. S. (2001). Half metallic magnets. *Phys. Today* 54, 39–44. doi: 10.1063/1.1381101

Singh, S., and Gupta, D. C. (2019). Lanthanum based quaternary Heusler alloys LaCoCrX (X = Al, Ga): hunt for half-metallicity and high thermoelectric efficiency. *Results Phys.* 13:102300. doi: 10.1016/j.rinp.2019.102300

Soluyanov, A. A., Gresch, D., Wang, Z., Wu, Q., Troyer, M., Dai, X., et al. (2015). Type-II Weyl semimetals. *Nature* 527, 495–498.

Son, Y., Cohen, M. L., and Louie, S. G. (2006). Half-metallic graphene nanoribbons. *Nature* 444, 347–349. doi: 10.1038/nature05180

Sun, G., Kurti, J., Rajczy, P., Kertesz, M., Hafner, J., and Kresse, G. (2003). Performance of the Vienna ab initio simulation package (VASP) in chemical applications. *J. Mol. Struct. Theochem.* 624, 37–45. doi: 10.1016/s0166-1280(02)00733-9

Szotek, Z., Temmerman, W. M., Svane, A., Petit, L., Stocks, G. M., and Winter, H. (2004). Half-metallic transition metal oxides. *J. Magn. Magn. Mater.* 272-276, 1816–1817. doi: 10.1016/j.jmmm.2003.12.818

Wang, X., Cheng, Z., Liu, G., Dai, X., Khenata, R., Wang, L., et al. (2017). Rare earth-based quaternary Heusler compounds MCoVZ (M = Lu, Y; Z = Si, Ge) with tunable band characteristics for potential spintronic applications. *IUCrJ* 4, 758–768. doi: 10.1107/s2052252517013264

Wang, X., Cheng, Z., Wang, J., Wang, L., Yu, Z., Fang, C., et al. (2016). Origin of the half-metallic band-gap in newly designed quaternary Heusler compounds ZrVTiZ (Z = Al, Ga). *RSC Adv.* 6, 57041–57047. doi: 10.1039/c6ra08600d

Wang, X., Dai, X. F., Wang, L., Liu, X., Wang, W., Wu, G. H., et al. (2015). Electronic structures and magnetism of Rh3Z (Z = Al, Ga, In, Si, Ge, Sn, Pb, Sb) with DO3 structures. *J. Magn. Magn. Mater.* 378, 16–23. doi: 10.1016/j.jmmm.2014.10.161

Wang, X., Ding, G., Cheng, Z., Yuan, H., Wang, X., Yang, T., et al. (2019). R3c-type LnNiO3 (Ln = La, Ce, Nd, Pm, Gd, Tb, Dy, Ho, Er, Lu) half-metals with multiple Dirac cones: a potential class of advanced spintronic materials. *IUCrJ* 6, 990–995. doi: 10.1107/s2052252519012570

Wu, R. Q., Peng, G., Liu, L., and Feng, Y. P. (2006). Wurtzite NiO: a potential half-metal for wide gap semiconductors. *Appl. Phys. Lett.* 89:082504. doi: 10.1063/1.2335970

Wu, W., Liu, Y., Li, S., Zhong, C., Yu, Z., Sheng, X., et al. (2018). Nodal surface semimetals: theory and material realization. *Phys. Rev. B* 97:115125.

Wu, X., Han, J., Feng, Y., Li, G. Q., Wang, C., Ding, G., et al. (2017). Half-metals and half-semiconductors in a transition metal doped SnSe2 monolayer: a first-principles study. *RSC Adv.* 7, 44499–44504. doi: 10.1039/c7ra07648g

Yan, L., Liu, P., Bo, T., Zhang, J., Tang, M., Xiao, Y., et al. (2019). Emergence of superconductivity in a Dirac nodal-line Cu2Si monolayer: ab initio calculations. *J. Mater. Chem. C* 7, 10926–10932. doi: 10.1039/c9tc03740c

Yi, X., Li, W. Q., Li, Z. H., Zhou, P., Ma, Z., and Sun, L. Z. (2019). Topological dual double node-line semimetals NaAlSi(Ge) and their potential as cathode material for sodium ion batteries. *J. Mater. Chem. C* 7, 15375–15381. doi: 10.1039/c9tc04096j

Young, S. M., and Kane, C. L. (2015). Dirac semimetals in two dimensions. *Phys. Rev. Lett.* 115, 126803–126803.

Zhang, M., Zhang, C., Wang, P., and Li, S. (2018). Prediction of high-temperature Chern insulator with half-metallic edge states in asymmetry-functionalized stanene. *Nanoscale* 10, 20226–20233. doi: 10.1039/c8nr07503d

Zhang, Y., Liu, Z. H., Wu, Z., and Ma, X. Q. (2019). Prediction of fully compensated ferrimagnetic spin-gapless semiconducting FeMnGa/Al/In half Heusler alloys. *IUCrJ* 6, 610–618. doi: 10.1107/s2052252519005062

Zhao, Z., Zhang, Z., and Guo, W. (2020). A family of all sp2-bonded carbon allotropes of topological semimetals with strain-robust nodal-lines. *J. Mater. Chem. C* 8, 1548–1555. doi: 10.1039/c9tc05470g

Zhou, P., Ma, Z., and Sun, L. Z. (2018). Coexistence of open and closed type nodal line topological semimetals in two dimensional B2C. *J. Mater. Chem. C* 6, 1206–1214. doi: 10.1039/c7tc05095j

Zou, Z. C., Zhou, P., Ma, Z., and Sun, L. Z. (2019). Strong anisotropic nodal lines in the TiBe family. *Phys. Chem. Chem. Phys.* 21, 8402–8407. doi: 10.1039/c9cp00508k

Žutic, I., Fabian, J., and Sarma, S. D. (2004). Spintronics: fundamentals and applications. *Rev. Mod. Phys.* 76, 323–410.

Conflict of Interest: The author declares that the research was conducted in the absence of any commercial or financial relationships that could be construed as a potential conflict of interest.